Electronic Supplementary Material (ESI) for CrystEngComm.

Supplementary information

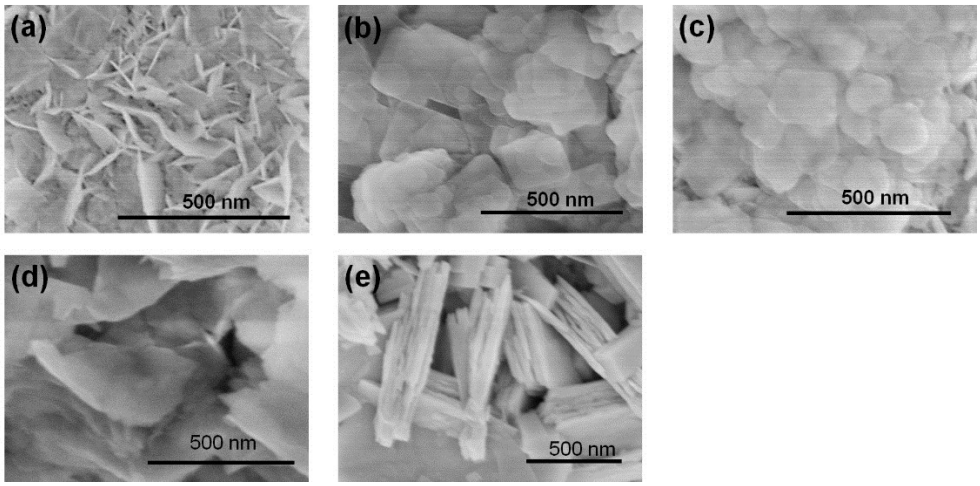

Figure S1. SEM images of products obtained at different concentration of added BPEI when fixing the concentration of PVP (7.14 g/L), KBr (2 mM), reaction temperature of 180°C and reaction time of 3 h in aqueous solution, (a) BOB-1, (b) BOB-2, (c) BOB-3, (d) BOB-4 and (e) BOB-5.

When increasing the concentration of added BPEI, the shapes of resulted products were evolved from assembled flower, 2D nanosheets, and stacked nanosheets (**Figure S1**).

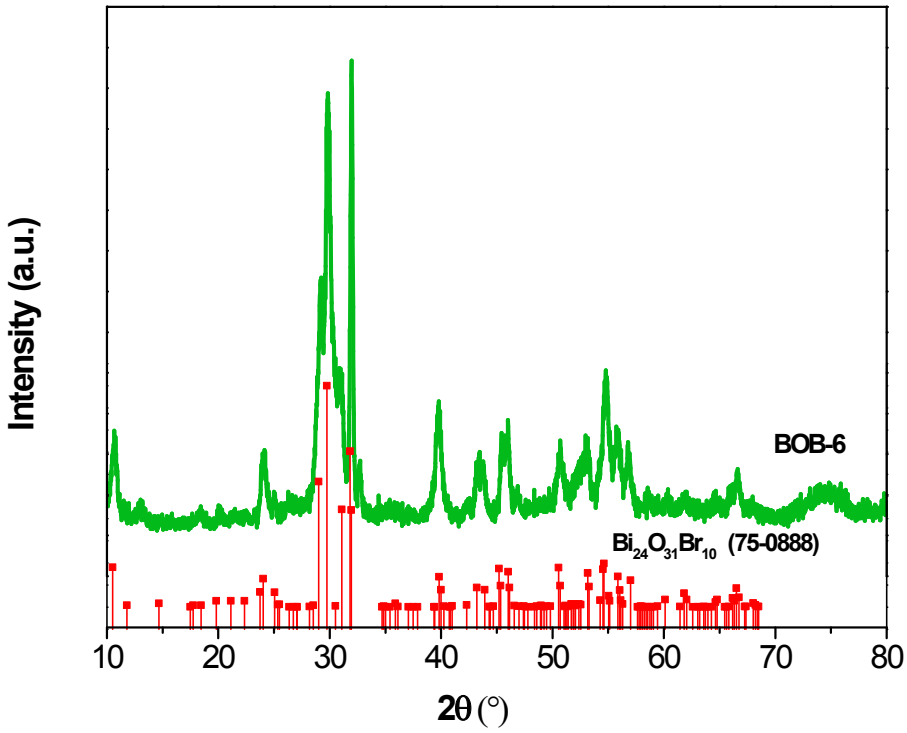

Figure S2. XRD pattern of BOB-6 by further raising up the concentration of added BPEI to 14.28 g/L when fixing the concentration of PVP at 7.14 g/L, KBr at 2 mM, reaction temperature of 180°C and reaction time of 3 h.

When increasing the concentration of BPEI to 14.28 g/L, all the characteristic peaks of final product were assigned to $Bi_{24}O_{31}Br_{10}$ (JCPDF No. 75-0888) (**Figure S2**).

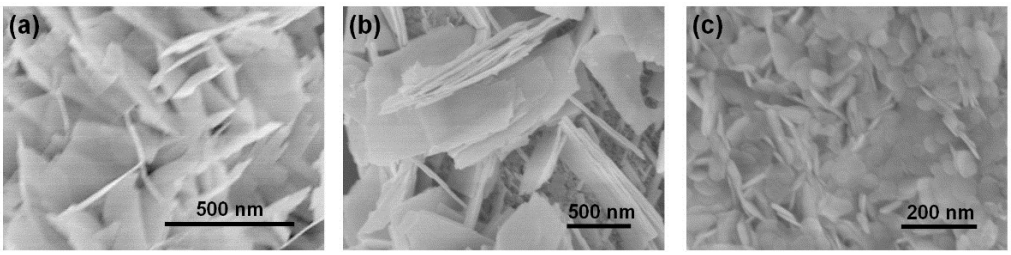

Figure S3. SEM images of products obtained at different concentration of KBr when maintaining the concentration of PVP at 7.14 g/L, BPEI at 3.57 g/L, reaction temperature of 180°C and reaction time of 3 h in aqueous solution, (a) BOB-7, (b) BOB-8, (c) BOB-9.

Altering the concentration of KBr, the morphology of final products was maintained in 2D nanosheets. But the size of these nanosheets was gradually decreased when increasing the concentration of Br^- (**Figure S3**).

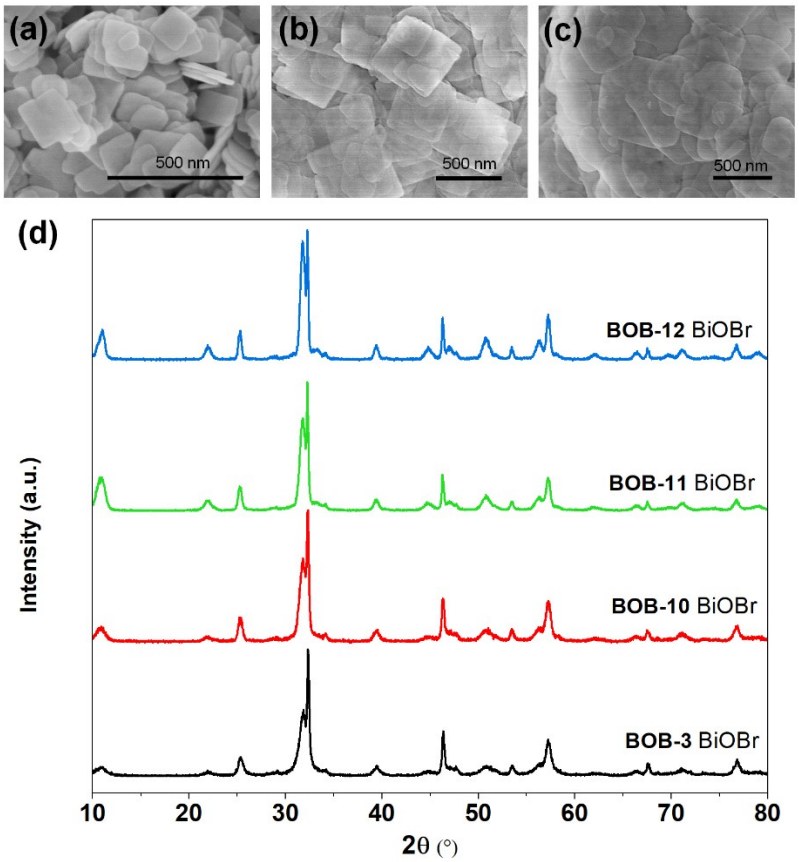

Figure S4. SEM images of products obtained in different solvent systems when keeping the concentration of PVP at 7.14 g/L, BPEI at 3.57 g/L and KBr at 2 mM, reaction temperature of 180°C and reaction time of 3 h in aqueous solution, (a) BOB-10, (b) BOB-11, (c) BOB-12. (d) XRD pattern of above samples.

Probably, the type of solvents plays a role in the protonation of BPEI. Then, the influence of solvents on BPEI protonating was investigated by selecting EG, aqueous solution of EG or G as solvent at certain concentration of BPEI (3.57 g/L) and PVP (7.14 g/L). Apparently, the shapes of resulted products were 2D nanosheets (BOB-3, BOB-10 to BOB-12) but with different size and shape edges (**Figure S4a** to **S4c**). All the products were indexed to pure tetragonal BiOBr (JCPDS No. 78-0348) (**Figure S4d**). Furthermore, the pH values of these experimental reactions were also closed to 4.0, indicating that the type of solvent had ignorable effect on the protonation of BPEI and phase transition.

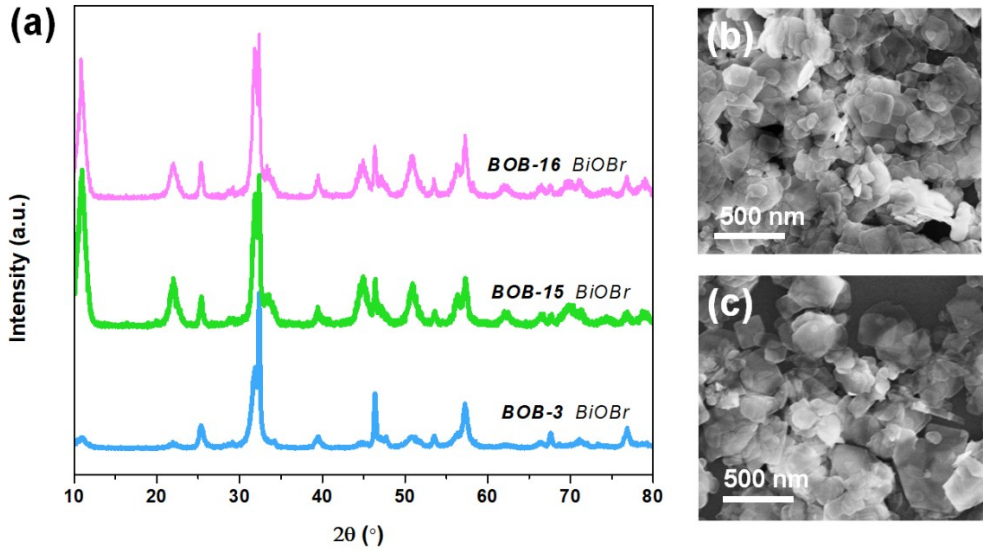

Figure S5. (a) XRD patterns of products obtained at different reaction time. SEM image of products prepared after (b) 12 h and (c) 24 h when maintaining the concentration of PVP at 7.14 g/L, BPEI at 3.57 g/L, reaction temperature of 180°C in aqueous solution.

Prolonging the reaction time from 3 h to 24 h (BOB-3, BOB-15 and BOB-16), the final products still maintained in tetragonal phase of BiOBr (JCPDS No. 78-0348, a = b =3.9233 Å, c = 8.105 Å, α = β = γ = 90 °) at these fixed conditions (**Figure S5a**). And, the intensity of (001) planes of BiOBr was increased when increasing the reaction time. Comparing with BOB-3 obtained at 3 h reaction time, the size of BOB-15 and BOB-16 nanosheets are gradually increased when prolonging the reaction time (**Figure S5b**, **Figure S1c** and **Figure S5**).

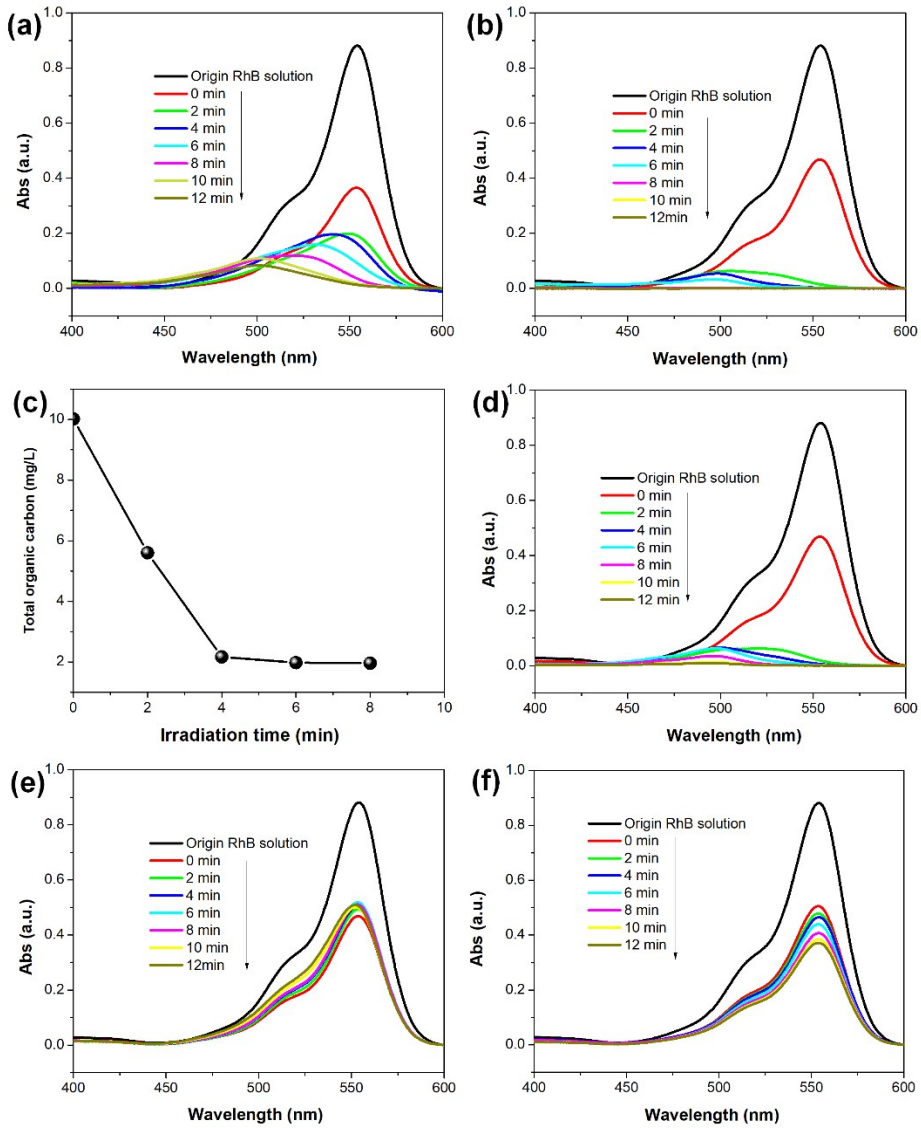

Figure S6. UV-vis absorption spectra of RhB (25 mg/L) over different photocatalysts, (a) BOB-3 and (b) BOB-5 under visible light irradiation. (c) Total organic carbon variation during the photocatalytic process. UV-vis absorption spectra of RhB (25 mg/L) over BOB-5 $Bi_4O_5Br_2$ nanosheets with adding scavengers of (d) IPA, (e) TEOA, and (f) AA.

According to the UV-vis absorption spectra of RhB over BOB-3 and BOB-5, the concentration of RhB decreased rapidly after exposure under the visible light (**Figure S6**). Furthermore, the RhB were photodegraded completely within 10 min for both photocatalysts (**Figure S6a** and **S6b**). During this photocatalytic process, the concentration of Total Organic Carbon (TOC) decreased gradually, indicating the RhB was degraded correspondingly (**Figure 6c**). Additionally, the photocatalytic performances of RhB over $Bi_4O_5Br_2$ NSs were different by

adding different scavengers. That was, the photocatalytic performance of RhB exhibited insignificant change by adding IPA (**Figure S6d**). However, in terms of adding TEOA, the RhB was unable to removed and even increased under visible-light irradiation due to the desorption from the surface of $Bi_4O_5Br_2$ NSs (**Figure S6e**). While, the RhB was slightly degraded by adding AA at same condition (**Figure S6f**). These results indicated that the $\bullet O_2$, and h^+ were the predominate roles for RhB degradation under visible-light irradiation.

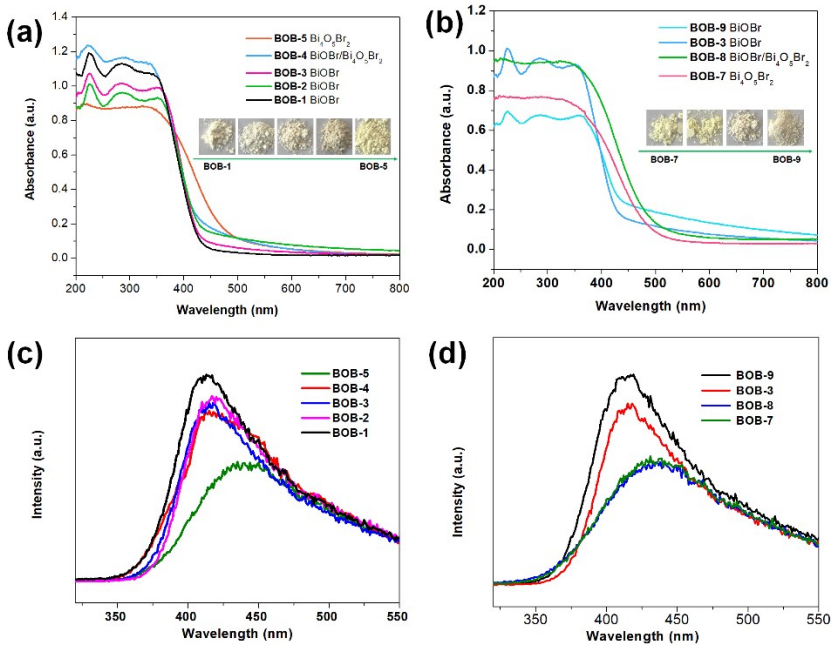

Figure S7. (a) DRS of samples prepared by adding different concentration of BPEI (inset with corresponding plots of $(\alpha h\gamma)^{1/2}$ vs. photon energy ($h\gamma$)). (b) DRS of samples prepared by adding different concentration of KBr (inset with corresponding plots of $(\alpha h\gamma)^{1/2}$ vs. $h\gamma$). Photoluminescence spectra of samples obtained by altering (c) the concentration of BPEI and (d) the concentration of Br^- with 310 nm excited wavelength.

The light absorption region and corresponding bandgap of different samples were estimated through the formula $(\alpha hv) = A(hv - Eg)^n$ (where α and hν are the absorption coefficient and photo energy, and n = 2 for BiOBr and $Bi_4O_5Br_2$ as an indirect semiconductor). Apparently, the light absorption range of prepared samples showed red-shift trend when increasing the concentration of BPEI. Then, the corresponding band gap of each sample was gradually decreased from ca. 2.85 to ca. 2.4 eV (**Figure S7a**). But, the light absorption range of samples obtained by increasing the concentration of Br^- presented inverse tendency of increasing BPEI, and the band gap of products was narrowed accordingly (**Figure S7b**).

Employing excited wavelength of 310 nm, the products showed different location and intensity of PL emission peaks (**Figure S7c–7d**). The products with monoclinic $Bi_4O_5Br_2$ present emission peak around 440nm, while products with tetragonal BiOBr showed emission peak around 410 nm. Furthermore, the intensity of $Bi_4O_5Br_2$ (such as, BOB-5, BOB-7 and BOB-8)

emission peak was lower than that of BiOBr, indicating the separation efficiency of $Bi_4O_5Br_2$ was higher than that of BiOBr.